Overtone spectra of C–H bonds and vibrational *ab initio* study of methoxy boranes

Carlos Manzanares I,[a] Dalat Walla, Randal Seburg, and Michael R. Wedlock
Department of Chemistry, Baylor University, Waco, Texas 76798

Carlos Gonzalez and H. Bernhard Schlegel
Department of Chemistry, Wayne State University, Detroit, Michigan 48202.

(Received 28 August 1990; accepted 16 May 1991)

The C–H overtone absorption spectra of $(CH_3O)_3B$ in liquid and gas phases are reported. The observed energies of the C–H stretching overtones corresponding to $\Delta v = 3$, 4, 5, and 6 (liquid) are obtained by conventional spectroscopy. The C–H overtones $\Delta v = 5$ and 6 (gas) are obtained by laser intracavity photoacoustic spectroscopy. Computer deconvolution of the gas-phase absorptions shows two bands at each overtone which are assigned as the overtones of nonequivalent C–H bonds. In general, for molecules in which a methyl group is directly attached to an oxygen atom, nonequivalent C–H bonds are produced due to the "*trans* effect." A different mechanism seems to occur in the case of the methyl groups in trimethylborate even though they are adjacent to an oxygen atom. In order to interpret the experimental results, *ab initio* molecular-orbital calculations were performed on $(CH_3O)BH_2$, $(CH_3O)_2BH$, and $(CH_3O)_3B$. Equilibrium geometries, vibrational frequencies, and infrared intensities were calculated at the Hartree–Fock level using the 3-21G split valence basis set. In the three molecules studied, the equilibrium conformation is such that the methyl groups have one C–H bond (C–H_a) in the plane of the molecule and *cis* to a B–O bond, and two equivalent C–H bonds located symmetrically above and below the plane of the molecule (C–H_b). In $(CH_3O)BH_2$, the in-plane C–H bond C–H_a is longer than the out-of-plane C–H bonds C–H_b (1.082 Å vs 1.0795 Å). This trend is reversed in the case of $(CH_3O)_3B$, where the C–H_a and C–H_b bond lengths are 1.0792 and 1.0807 Å, respectively. The situation is more complicated in the case of the molecule $(CH_3O)_2BH$, where in one methyl group the C–H_a bond is shorter than the C–H_b bond (1.0794 Å vs 1.0802 Å), while in the other methyl group the corresponding C–H_a bond is longer than the C–H_b bond (1.0829 Å vs 1.0802 Å). The nature of the difference in the C–H bond lengths is studied and discussed in terms of group orbital interactions in both, the σ and π systems. In addition, a correlation between the C–H bond length, the corresponding C–H stretching force constant, and the vibrational frequency is discussed based on vibrational frequency calculations performed on the deuterated species $(CHD_2O)_nBH_{3-n}$ for $n = 1$, 2, 3 in cases where the isolated C–H was considered to be the in-plane C–H_a or the out-of-plane C–H_b.

I. INTRODUCTION

The calculated molecular structures of methoxyborane $(CH_3O)BH_2$, dimethoxyborane $(CH_3O)_2BH$, and trimethylborate $(CH_3O)_3B$ in their equilibrium conformations are shown in Figs. 1–3. The molecular structure of trimethylborate has been obtained by Gundersen[1] using electron diffraction in the gas phase. Gundersen found that the $B(OC)_3$ skeleton is on one plane and has symmetry C_{3h}. In the most-stable geometric conformation, two hydrogen atoms in the methyl groups are above and below the plane of the molecule while the other is in the plane of the molecule as shown in Fig. 3. In this conformation, an in-plane C–H bond (C–H_a) and an O–B bond are *cis* with respect to each other. The vibrational spectra and a normal coordinate analysis[2] based on the molecular structure given by Gundersen support this conformation. It is suspected that the rotational barrier of the methyl groups is quite low.[1,2] Kawashima, Takeo, and Matsumura[3] have conducted a microwave study of methoxyborane (CH_3OBH_2) and partially deuterated (CHD_2OBH_2) samples. The microwave studies and *ab initio* molecular-orbital calculations of the molecule confirm a conformation (see Fig. 1) of the methyl group similar to the one found for $(CH_3O)_3B$ in which an in-plane C–H bond is *cis* to an O–B bond. The rotational barrier of CH_3 in CH_3OBH_2 is estimated to be 3.09 kJ/mol.

The influence of conformation on individual C–H bond strengths was initially demonstrated by McKean,[4] who measured the fundamental frequencies of compounds which are fully deuterated except for a single C–H bond. Overtone studies by Swofford and co-workers[5,6] have also distinguished nonequivalent C–H bonds in methyl groups. If the methyl group is in a conformationally anisotropic environment created by an adjacent heteroatom (N, O, S), the IR spectra of the partially deuterated molecule or the overtone spectra of the normal molecule consist of two distinct bands for each nonequivalent C–H bond. The cause of the nonequivalence has been attributed to the lone-pair *trans* effect. It

[a] To whom correspondence should be addressed.

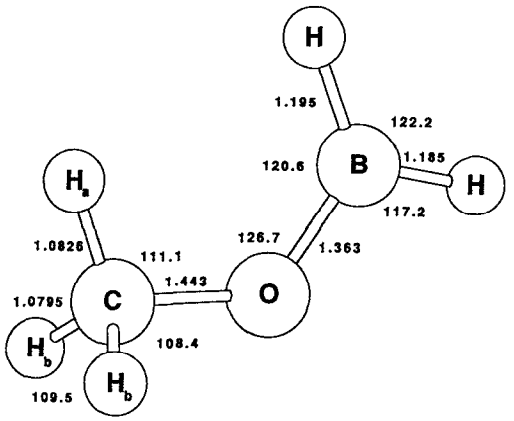

FIG. 1. Equilibrium geometry for $(CH_3O)BH_2$ calculated at the HF/3-21G level.

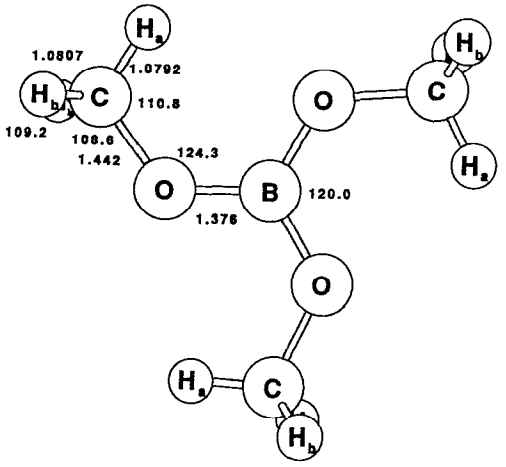

FIG. 3. Equilibrium geometry for $(CH_3O)_3B$ calculated at the HF/3-21G level.

has been suggested[4,7,8] that heteroatoms like N or O with lone-pair electrons, donate electron density into an antibonding orbital of a *trans* C–H group. This effect induces a weakening of the C–H bond *trans* to the lone pair. In molecules in which the methyl group is adjacent to a multiple bonded atom like C=C or C=O; the out-of-plane C–H bonds in the molecule are weakened by hyperconjugation.[4,9] According to this, a nonbonding electron-pair repulsion between the π electrons and the C–H out-of-plane bonding pairs occurs which weakens the out-of-plane C–H bonds.

Structural studies of compounds of the .type CH_3–O–R,[10–14] with R as $-CH_3$, –CHO, –NO, $-NO_2$, –Cl, etc., have shown that the conformation of the methyl group is such that there is an in-plane C–H bond which is *trans* to the O–R bond and there are two C–H bonds oriented symmetrically above and below the molecular plane and each is *trans* to an oxygen lone pair. It is expected that the out-of-plane C–H bonds are weaker than the in-plane C–H bond due to the *trans* effect. In compounds with methyl groups adjacent to multiple bonded atoms C=X (X as O or C) the methyl group conformation is such that the in-plane C–H bond is *cis* to the C=X bond and there are two out-of-plane C–H bonds which are weakened by hyperconjugation.

The conformation of a methyl group in compounds CH_3–O–B is different from the conformation of a methyl group in compounds CH_3–O–R. The in-plane C–H bond is *cis* with respect to the O–B bond in the former and it is *trans* in the latter. Also, the barrier of internal rotation of a methyl group in CH_3–O–B is smaller than in other compounds (CH_3–O–R).[11–13] Because of this, $(CH_3O)_3B$ is a particularly interesting molecule to study. On the one hand, the out-of-plane C–H bonds are not *trans* to the oxygen lone pairs and the only (if any) *trans* effect that could occur is with the in-plane (slightly tilted) C–H bond. On the other hand, the boron atom is electron deficient and a certain degree of π bond is usually assigned[1–3] to the O–B bond. The present study was initiated to find which interactions are more important to determine the energy of the C–H overtone bands in this molecule.

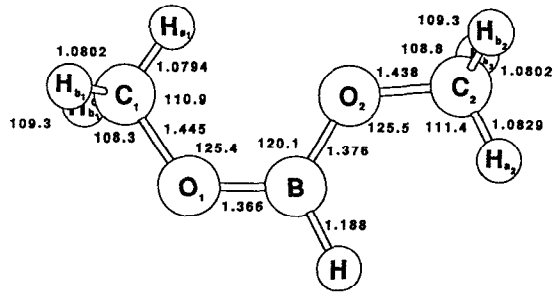

FIG. 2. Equilibrium geometry for $(CH_3O)_2BH$ calculated at the HF/3-21G level.

In the present work the C–H overtone spectra of liquid trimethylborate have been studied using standard absorption methods for transitions with $\Delta v = 3$, 4, 5, and 6. The C–H overtone spectra in the gas phase were obtained for transitions with $\Delta v = 5$ and 6 using laser intracavity photoacoustic spectroscopy. The gas-phase overtone bands for $\Delta v = 5$ and 6 have been computer deconvoluted to assign overtone and combination band absorptions. Deconvolution of gas-phase overtone bands shows bands which are associated with different C–H absorptions within the same methyl group. The effect of the O–B bond on the intensity and position of the bands is discussed. Results are interpreted in terms of the local-mode description of vibrational overtones[15–17] from which local-mode harmonic frequencies (ω_e) and anharmonicities ($\omega_e x_e$) have been calculated. Tentative assignments of combination bands are also presented. In order to assign the absorptions due to the different C–H bonds and to explain the experimental results, *ab initio* molecular-orbital calculations were performed on the three related molecules, $(CH_3O)BH_2$, $(CH_3O)_2BH$, and $(CH_3O)_3B$. Equilibrium geometries, vibrational frequencies, and infrared intensities were calculated at the Hartree–Fock level using the 3-21G split-valence basis set. Experimental studies on the molecules $(CH_3O)BH_2$ and $(CH_3O)_2BH$ were not done because of their unstability.

The compound $(CH_3O)BH_2$ is an intermediate in the reaction of diborane with methanol and its lifetime is several seconds.[3] The compound $(CH_3O)_2BH$ is more stable than $(CH_3O)BH_2$ but decomposes in several days forming trimethylborate and diborane.[18]

II. EXPERIMENT

Trimethylborate (Aldrich, 99%) samples were further purified by freeze-pump-thaw cycles before use. The fundamental spectrum around the C–H absorption was obtained with a Nicolet 20 DX Fourier transform infrared spectrophotometer. The first overtone region was recorded with a Cary 14 spectrophotometer and a 2.4 mm path-length cell. The remaining spectra around the $\Delta v(CH) = 3$, 4, 5, and 6 were obtained with a Perkin-Elmer 330 spectrophotometer in the near-infrared and visible regions. A 1 cm path-length cell was used in the region of the second and third overtones, and a 5 cm cell in the region around the fourth and fifth overtones. Improved signal-to-noise ratios were obtained for $\Delta v(CH) > 5$ by averaging 20 scans of the spectral region using a Perkin-Elmer infrared data station.

Gas-phase laser photoacoustic spectra were obtained for the $\Delta v = 5$ and 6 C–H stretching vibrations using a cell mounted within the cavity of a cw dye laser (Coherent 599-01) with high-reflectance optics, pumped with an argon-ion laser (Laser Ionics 554A). The photoacoustic cell is 1 cm diameter and 20 cm long, made of Pyrex tubing with quartz windows mounted at Brewster's angle. The photoacoustic signal is detected by a Knowles BT1759 electret microphone attached to a flange mounted at the midpoint of the cell. The ion laser pump beam is modulated by a mechanical chopper at a frequency of 100 Hz. Signals from the microphone are amplified and processed by an Ithaco lock-in amplifier (3962A). The intracavity dye laser power is monitored with a photodiode which detects a reflection off of the Brewster angle window of the cell. This signal is fed to a Stanford lock-in amplifier (SR510). Normalization of the photoacoustic spectra is achieved by ratioing the output signals from both lock-in amplifiers. Wavelength tuning (1.0 cm^{-1} bandwidth) of the dye laser is accomplished with a stepper-motor-driven birefringent filter. A microcomputer system controls the dye-laser wavelength scan and digitizes and stores the normalized signals for further analysis. Absolute calibration of laser lines was achieved obtaining the optogalvanic spectra of hollow cathode lamps filled with argon (700–800 nm) or neon (600–700 nm). The tuning ranges of the laser dyes are as follows: Pyridine 2 (13 000–14 500 cm^{-1}) and Rhodamine 610 (14 800–16 500 cm^{-1}) pumped by the blue green lines of the Ar^+ laser. In each case a high-reflectance ($> 99.7\%$) dye laser output coupler is used to increase the intracavity laser power. All experiments were performed at 20 ± 2 °C.

III. RESULTS

Figure 4 shows the absorption spectrum around the region of the overtones $\Delta v(CH) = 3$ and 4 of neat liquid trimethylborate. Similarly, Fig. 5 shows the absorption spectrum in the region around $\Delta v(CH) = 5$ and 6. Figure 6 depicts the fourth overtone spectra ($\Delta v = 5$) in the C–H stretching region for gaseous $(CH_3O)_3B$ and Fig. 7 the fifth

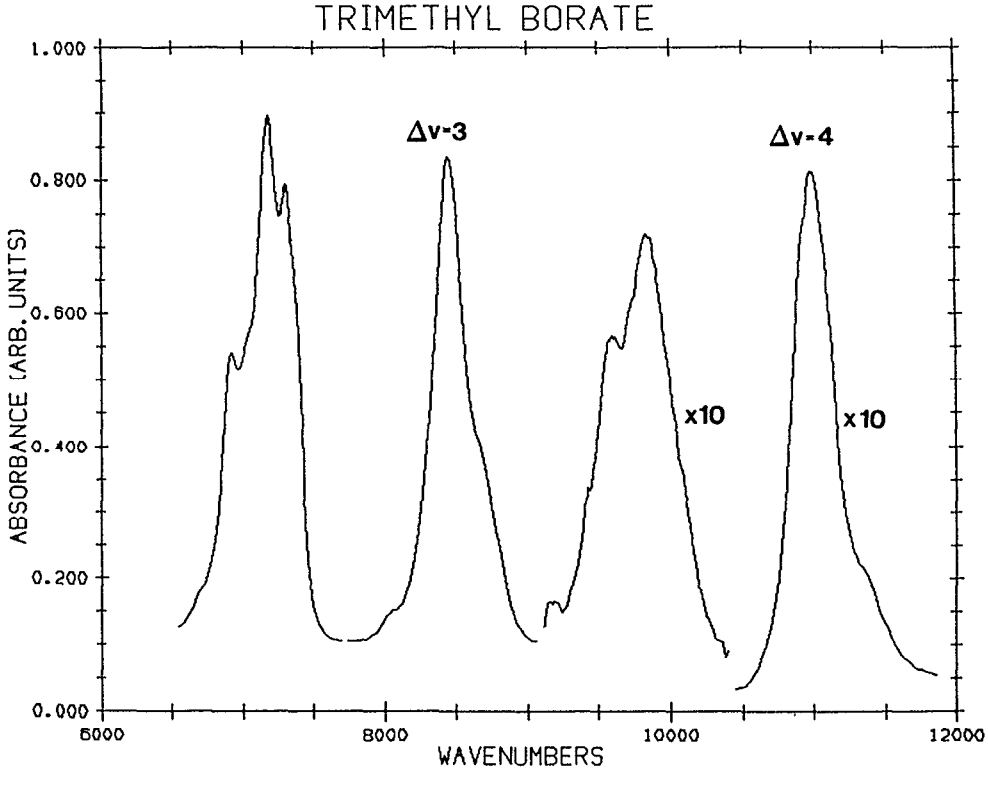

FIG. 4. Overtone spectrum of room-temperature, liquid-phase $(CH_3O)_3B$ around the $\Delta v(CH) = 3$, 4 region. The cell path length was 1 cm.

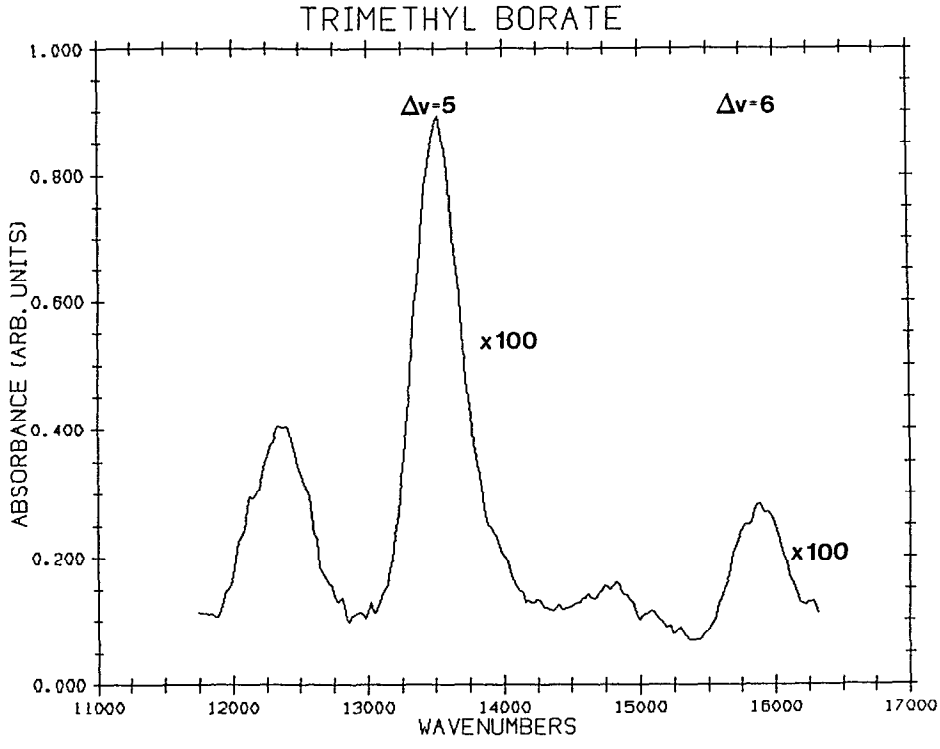

FIG. 5. Overtone spectrum of room-temperature, liquid-phase $(CH_3O)_3B$ around the $\Delta v(CH) = 5$, 6 region. The cell path length was 5 cm.

overtone ($\Delta v = 6$). The pressures inside the cell were 23 and 98 Torr, respectively. The liquid spectra were digitized and fed to a Digital VAX computer and replotted on a linear wave-number scale. The bands around the $\Delta v = 5$ and 6 region originally had a rising base line due to instrumental transmission changes of the spectrophotometer. This rising base line was corrected by computer linearization and normalization of the base line.[19] The principal overtones $\Delta v = 3$, 4, and 5 were computer deconvoluted to obtain the position of the peaks and the full width at half maximum (FWHM) of the local-mode absorption bands. The gas-phase overtones $\Delta v(CH) = 5$ and 6 were also computer deconvoluted. Deconvolutions were performed with programs developed by Jones and Pitha[20] and modified to run in the VAX computer. The digitized data of the gas-phase overtones were fed to the computer along with the number of peaks to be used in the analysis, a set of approximate absorbances, peak positions, and bandwidths. The deconvolution program uses a nonlinear least-squares method to optimize the parameters given. The program terminates after a successful fit of the input data by the generated function. Each individual peak was fitted with a Lorentzian band shape. The bands are defined by the maximum peak absorbance, the wave number of the maximum, the full width at half

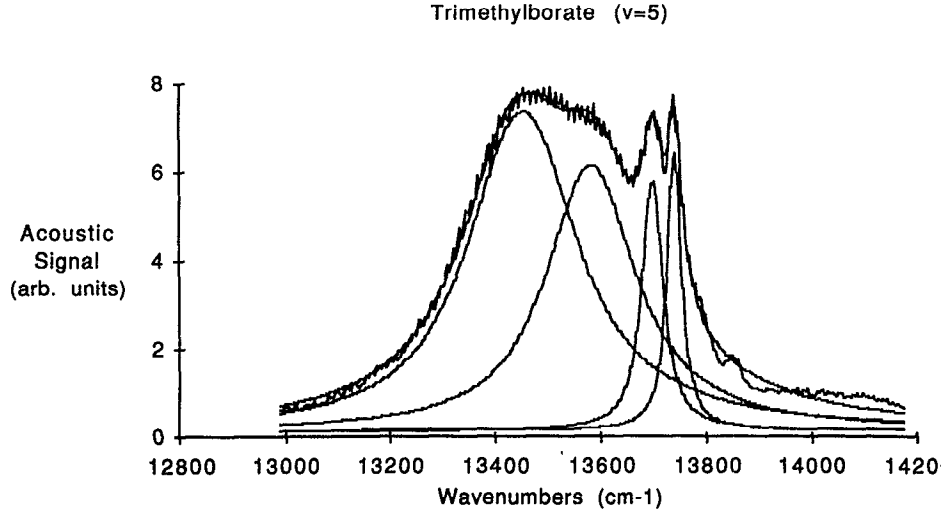

FIG. 6. Intracavity photoacoustic spectrum of the $\Delta v(CH) = 5$ region of $(CH_3O)_3B$. The sample pressure was 23 Torr. Temperature 20 ± 2 °C. Computer deconvolution shows the component bands.

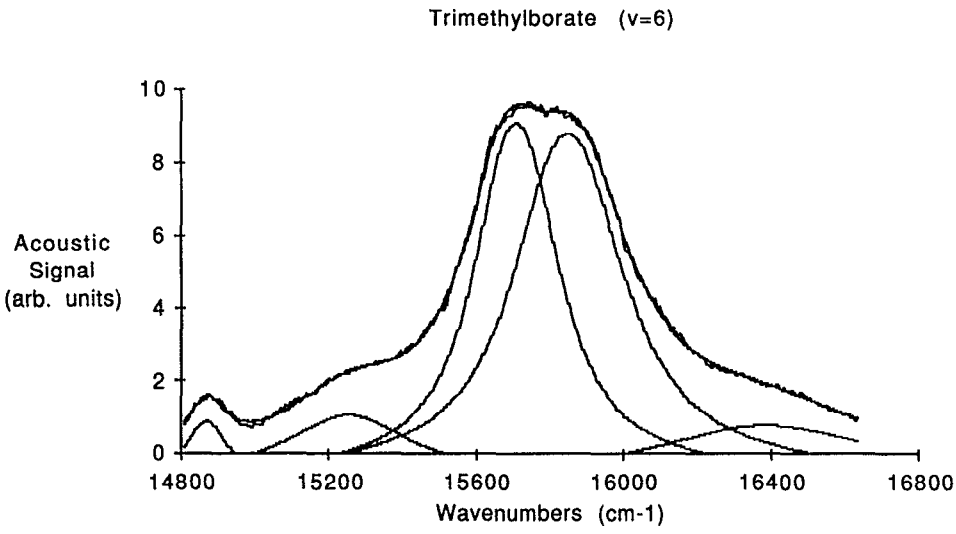

FIG. 7. Intracavity photoacoustic spectrum of the $\Delta v(CH) = 6$ region of $(CH_3O)_3B$. The sample pressure was 98 Torr. Temperature 20 ± 2 °C. Computer deconvolution shows the component bands.

maximum, and the base-line constant. The calculated spectra were then plotted with the experimental spectra so that a visual comparison could be made to insure the quality of the fit. The discrepancy between the calculated and the experimental spectra was minimized with the program.

IV. DISCUSSION

Due to uncertainties in the assignments, and to understand the interactions that affect the C–H bonds of the methyl groups, *ab initio* molecular-orbital calculations were performed on $(CH_3O)_3B$. For completeness and in order to explain the nature of the interactions, the related molecules $(CH_3O)BH_2$ and $(CH_3O)_2BH$ were also included in the calculation. The GAUSSIAN 86 system of programs[21] was used. All the equilibrium geometries were fully optimized at the Hartree–Fock level with analytical gradient methods[22] using the 3-21G split-valence basis set.[23] Vibrational frequencies and intensities were calculated from analytical second derivatives[24] at the same level of theory using the 3-21G optimized geometries.

A. Molecular structures

Figures 1–3 show the optimized structures of CH_3OBH_2, $(CH_3O)_2BH$, and $(CH_3O)_3B$, respectively. In their equilibrium conformation, the methyl groups in these molecules have one C–H bond (C–H_a) in the plane of the molecule and *cis* to a B–O bond, and two equivalent C–H bonds located symmetrically above and below the plane of the molecule (C–H_b).

For methoxyborane, CH_3OBH_2, the C–H_a bond is longer than the pair of equivalent C–H_b bonds (1.0826 Å vs 1.0795 Å; see Fig. 1). Correspondingly, the in-plane bond, CH_a, has a smaller stretching force constant than the out-of-plane bond C–H_b (5.80 mdyn/Å vs 5.91 mdyn/Å; see Table I). The structure of CH_3OBH_2 has been determined from microwave spectra by Kawashima, Takeo, and Matsumura.[3,25] The calculated C–O and B–O bond lengths are slightly larger than the experimental values (1.443 Å vs 1.425 Å for C–O and 1.363 Å vs 1.352 Å for the B–O bond).

Dimethoxyborane, $(CH_3O)_2BH$, exhibits two different methyl groups with different in-plane (C–H_{a1} and C–H_{a2}) and out-of-plane (C–H_{b1} and C–H_{b2}) C–H bonds (see Fig. 2). For one methyl group, the in-plane bond is shorter than the out-of-plane bond (C–H_{a1}: 1.0794 Å vs C–H_{b1}: 1.0802 Å), whereas the situation is reversed in the other methyl group (C–H_{a2}: 1.0829 Å vs C–H_{b2}: 1.0802 Å). As shown in Table I, the variations in the C–H stretching force constants are also reversed for the two methyl groups (5.95 and 5.78 mdyn/Å for C–H_{a1} and C–H_{b1}, vs 5.78 and 5.88 mdyn/Å for C–H_{a2} and C–H_{b2}). Since both methyl groups are bonded to oxygens which are bonded to the boron, the differences in the C–H bonds cannot be explained simply by inductive interactions with the adjacent oxygen and/or the boron. More subtle changes in interactions appear to be responsible, as discussed below.

The optimized geometry of the trimethyl borate, $(CH_3O)_3B$, is shown in Fig. 3. In agreement with the results of electron-diffraction experiments,[1] the calculated structure has C_{3h} symmetry. The calculated B–O bond distance is 0.009 Å longer than the experimental value (1.376 Å vs 1.367 Å), while the calculated C–O distance is 0.018 Å longer than the value found experimentally by Gundersen[1] (1.442 Å vs 1.424 Å). The *ab initio* calculations indicate that there are three equivalent in-plane C–H bonds (C–H_a) and three equivalent pairs of out-of-plane C–H bonds (C–H_b) (see Fig. 3). The C–H_a bonds are shorter than the out-of-plane C–H_b bonds (1.0792 Å vs 1.0807 Å), and correspondingly the stretching force constant for the C–H_a is larger than for C–H_b (5.97 and 5.85 mdyn/Å, respectively).

B. Calculated rotational barriers, frequencies, and intensities

For $(CH_3O)_nBH_{3-n}$, the barriers for rotation of a single methyl group are all calculated to be ca. 3.34 kJ/mol at the HF/3-21G level. This agrees well with the experimental barrier of 3.09 kJ/mol found by Kawashima, Takeo, and

TABLE I. Calculated bond lengths R(C–H), force constants $K_{C\text{-}H}$, frequencies, and infrared intensities for the different C–H stretchings in CH_3OBH_2, $(CH_3O)_2BH$, and $(CH_3O)_3B$. Subscript a indicates in-plane C–H bond. Subscript b indicates out-of-plane C–H bond.

Molecule	R(C–H) (Å)	$K_{C\text{-}H}$ (mdyn/Å)	Frequency (cm^{-1})	Intensity (KM/mol)
CH_3OBH_2				
CH_aD_2OBH2	1.0826	5.80	3242	30.32
CH_bD_2OBH2	1.079	5.91	3276	34.30
$(CH_3O)_2BH$				
$CH_{a1}D_2OBOCD_3$	1.0794	5.95	3286	16.04
$CH_{b1}D_2OBOCD_3$	1.0802	5.88	3266	44.84
$CD_3OBOCH_{a2}D_2$	1.0829	5.78	3238	34.77
$CD_3OBOCH_{b2}D_2$	1.0802	5.88	3265	41.92
$(CH_3O)_3B$				
$CH_aD_2OB(OCD_3)_2$	1.0792	5.97	3289	14.98
$CH_bD_2OB(OCD_3)_2$	1.0807	5.85	3258	49.38

Matsumura[3] for CH_3OBH_2. Table II lists the harmonic frequencies calculated at the HF/3-21G level for CH_3OBH_2, $(CH_3O)_2BH$, and $(CH_3O)_3B$, respectively. In the case of $(CH_3O)_3B$, the experimental frequencies obtained by Rogstad *et al.*[2] are also listed. In general, the calculated frequencies are ca. 11% higher than the experimental, due to basis sets truncation, correlation effects, and neglect of anharmonicity corrections.[26]

For CH_3OBH_2, $(CH_3O)_2BH$, and $(CH_3O)_3B$, stretching frequencies and IR intensities for isolated in-plane (C–H_a) and out-of-plane (C–H_b) bonds were calculated by replacing all of the other hydrogens by deuterium (Table I). In CH_3OBH_2, the in-plane C–H stretching is lower in frequency than the out-of-plane C–H, as expected from the fact that the C–H_a bond is longer than the C–H_b bond. For $(CH_3O)_2BH$ there are two nearly equal out-of-plane C–H_b stretches (3265 and 3266 cm^{-1}). However, the two in-plane C–H stretches are quite different, one lower than the out-of-plane modes (3238 cm^{-1}) and the other higher (3286 cm^{-1}). This parallels the difference in bond lengths. The relative ordering of the C–H stretching frequencies in $(CH_3O)_3B$ is the opposite of CH_3OBH_2; the higher-frequency band (3289 cm^{-1}) corresponds to the in-plane C–H_a stretch, while the lower-frequency band (3258 cm^{-1}) corresponds to the out-of-plane C–H_b stretch. In all cases the calculated IR intensities for the in-plane stretches are equal to or lower than the out-of-plane stretches in the same molecule. For $(CH_3O)_3B$ and C–H_{a1} $(CH_3O)_2BH$, the in-plane stretch is only 1/3–1/2 as intense as the other C–H stretches. The same level of calculations for methanol as well as overtone calculations of methanol by Sage[27] also predict the in-plane stretch to be ca. + 1/2 the intensity of the out-of-plane stretch.

TABLE II. Calculated vibrational frequencies for CH_3OBH_2, $(CH_3O)_2BH$, and $(CH_3O)_3B$.

Molecule	Frequencies (cm^{-1})[a]
CH_3OBH_2	136, 375, 417, 973, 1088, 1157 1268, 1276, 1350, 1482, 1645 1676, 1687, 2693, 2799, 3211 3281, 3297.
$(CH_3O)_2BH$	58, 95, 135, 185, 290, 331, 607 974, 1003, 1041, 1227, 1260 1274, 1277, 1300, 1383, 1508 1633, 1674, 1681, 1687, 1689 1692, 2776, 3207, 3222, 3271 3285, 3285, 3304.
$(CH_3O)_3B$	55(165), 60(102), 96 157(230) 183(187), 322(317), 554(521) 699(667), 750(729), 1099(1041) 1220(1125), 1276(1115), 1276(1165) 1289(1204), 1334(1183), 1503(1365) 1627(1450), 1669(1468), 1689(1470) 1691(1489), 1692(1485), 1692(1510) 3218(2882), 3220(2867), 3277(2974) 3278(2964), 3305(2942), 3305(2964)

[a] Values in parentheses refer to experimental frequencies.

C. Overtone assignments for $(CH_3O)_3B$

Based on the *ab initio* calculations of energy separation (31 cm^{-1}) and bond-length difference [ΔR(C–H) = 0.0015 Å] of C–H_a and C–H_b bonds for $(CH_3O)_3B$, it is reasonable to expect that the C–H_a and C–H_b peaks are unresolved in the liquid phase. In Figs. 4 and 5, corresponding to the liquid spectra, a band on the low-energy side of each overtone can be observed. This band whose maximum decreases in intensity when the $\Delta\nu$(CH) increases is a combination band which involves in each case, an overtone and the B–O stretching vibration. Table III presents experimental and calculated peak positions, assignments, and linewidths for selected transitions of the liquid- and gas-phase spectra. The fundamental frequencies[2] that appear to be involved in combination bands with overtones are the $\nu_{19} = 1364\ cm^{-1}$ which is the B–O stretch; the CH_3 rocking fundamental $\nu_{26} = 1165\ cm^{-1}$; the CH_3 bending $\nu_{17} = 1510\ cm^{-1}$; and the CH_3 stretching frequencies $\nu_1 = 2942\ cm^{-1}$, $\nu_2 = 2867\ cm^{-1}$, $\nu_9 = 2964\ cm^{-1}$,

TABLE III. Experimental and calculated overtone frequencies, transition assignments, and linewidths (FWHM) of C–H stretching modes of $(CH_3O)_3B$.

Quantum number Δv(CH)	Peak position (cm^{-1}) Expt.	Calc.	FWHM (cm^{-1})	Assignment
Liquid-phase overtones				
2	5 776	5 758[a]		$2\nu_{CH}$
	5 901	5 906		$\nu_1 + \nu_9$
	6 919	6 941		$2\nu_{CH} + \nu_{26}$
	7 130	7 140		$2\nu_{CH} + \nu_{19}$
	7 300	7 286		$2\nu_{CH} + \nu_{17}$
3	8 445	8 458[a]	250	$3\nu_{CH}$
	8 690	8 658	210	$2\nu_{CH} + \nu_{16}$
	9 595	9 610		$3\nu_{CH} + \nu_{26}$
	9 826	9 809		$3\nu_{CH} + \nu_{19}$
4	10 993	11 039[a]	324	$4\nu_{CH}$
	11 350	11 327	370	$3\nu_{CH} + \nu_{16}$
	12 362	12 357		$4\nu_{CH} + \nu_{19}$
5	13 506	13 501[a]	393	$5\nu_{CH}$
	13 847	13 860	529	$4\nu_{CH} + \nu_2$
6	15 800	15 843[a]		$6\nu_{CH}$
Gas-phase overtones				
5	13 452		235	$5\nu_b$
	13 581		196	$5\nu_a$
	13 718			doublet
6	14 870	14 902		$5\nu_b + \nu_4$
	15 251	15 222		$5\nu_b + \nu_7 + \nu_{21}$
	15 709		259	$6\nu_b$
	15 850		327	$6\nu_a$
	16 385	16 394		$5\nu_b + \nu_1$

[a] Calculated from Eq. (1).

$\nu_{15} = 2953\ cm^{-1}$, $\nu_{16} = 2882\ cm^{-1}$, and $\nu_{24} = 2974\ cm^{-1}$. Transitions around $\Delta v = 2$ (not shown) are assigned as $2\nu_{CH}$ at 5776 cm^{-1} and $\nu_1 + \nu_9$ at 5901 cm^{-1}. The band on the low-energy side of $\Delta v = 3$ in Fig. 4 shows three peaks: one at 6919 cm^{-1} assigned as the combination band $2\nu_{CH} + \nu_{26}$, another at 7130 cm^{-1} assigned as $2\nu_{CH} + \nu_{19}$, and the one at 7300 cm^{-1} is assigned as $2\nu_{CH} + \nu_{17}$. The $\Delta v = 3$ spectrum shows the main transition at 8445 cm^{-1} ($3\nu_{CH}$), with a shoulder at 8690 cm^{-1} which is the combination band ($2\nu_{CH} + \nu_{16}$). The other band on the high-energy side of $\Delta v = 3$ shows two peaks, one at 9595 cm^{-1} assigned as $3\nu_{CH} + \nu_{26}$ and another at 9826 cm^{-1} that corresponds to the combination $3\nu_{CH} + \nu_{19}$. The $\Delta v = 4$ region shows the main band at 10 993 cm^{-1} ($4\nu_{CH}$) and a shoulder at 11 350 cm^{-1} ($3\nu_{CH} + \nu_{16}$). In Fig. 5 the band at 12 362 cm^{-1} is assigned as the combination band $4\nu_{CH} + \nu_{19}$. The region around $\Delta v = 5$ shows the main peak at 13 506 cm^{-1} assigned as $5\nu_{CH}$, the deconvoluted band shows another absorption at 13 487 cm^{-1} which is assigned as $4\nu_{CH} + \nu_2$. The weak absorption with a peak at 15 800 cm^{-1} is the $6\nu_{CH}$ overtone of the liquid.

Fundamentals and overtones of nonequivalent C–H bonds in molecules with similar bond-length difference as $(CH_3O)_3B$ have been obtained.[4,28] For example, in $(CH_3)_3P$ with ΔR(C–H) = 0.0037 Å and in $(CH_3)_3As$ with ΔR(C–H) = 0.0026 Å two separated bands have been obtained for $\Delta v = 5$, 6, and 7 of the gas-phase spectra.[30] In each case the two bands were observed because of the very narrow linewidths of the C–H_a and C–H_b absorptions. The gas-phase results shown in Figs. 6 and 7 for transitions with Δv(CH) = 5 and 6 present very wide bands which only after deconvolution show the two absorption bands that could be associated with C–H_a and C–H_b bonds. There is also in Fig. 6 an unknown doublet that overlaps the main absorption on the high-energy side and could be a combination band. The band with a maximum around 13 452 cm^{-1} is assigned as $5\nu_b$. The other absorption at 13 581 cm^{-1} is assigned as $5\nu_a$. The spectrum shown in Fig. 7 corresponds to the $\Delta v = 6$ transitions in the gas phase. The doublet is not present in this spectrum but the two main transitions still overlap. The component bands are at 15 706 and 15 851 cm^{-1}. They are assigned as $6\nu_b$ and $6\nu_a$, respectively. Other absorptions in

this spectrum are assigned as the combination bands $5\upsilon_b + \upsilon_4$ at 14 870 cm^{-1}, $5\upsilon_b + \upsilon_7 + \upsilon_{21}$ at 15 251 cm^{-1}, and $5\upsilon_b + \upsilon_1$ at 16 385 cm^{-1}.

D. Harmonic frequencies and anharmonicities for $(CH_3O)_3B$

Local modes[14–16] are used to interpret the overtone spectra in the way that normal modes have been used to systematize fundamental vibrational spectra. Absorption peak energies in the local-mode description are fit by the one-dimensional anharmonic-oscillator equation:[15]

$$\Delta E_\upsilon = (\omega_e - \omega_e x_e)\upsilon - \omega_e x_e \upsilon^2, \quad (1)$$

where ω_e and $\omega_e x_e$ are the mechanical frequency and anharmonicity constants, respectively. The transition energies ΔE_υ are given in Table III as the overtones $\upsilon\upsilon_{CH}$ with $\upsilon = 1$–6 of the liquid. A Birge–Sponer[29] plot using Eq. (1) gives the values $\omega_e - \omega_e x_e = (2981 \pm 13)$ cm^{-1} and $\omega_e x_e = (56 \pm 3)$ cm^{-1} for the C–H oscillators of the liquid. The individual C–H_b and C–H_a parameters were not obtained, because the transitions corresponding to the C–H_b and C–H_a bonds are unresolved in the liquid. In the gas phase, the bands due to the nonequivalent C–H bonds are wide and unresolved, but it is possible to see how they overlap. The bands of the two types of oscillators were obtained after computer deconvolution for $\Delta\upsilon = 5$ and 6. The values of ΔE given in Table III (gas-phase overtones) for $\Delta\upsilon = 5$ and 6 and Eq. (1), are used to estimate the harmonic frequencies and anharmonicities in the gas phase. The estimated values are $\omega_e - \omega_e x_e = 3089\ cm^{-1}$ and $\omega_e x_e = -75\ cm^{-1}$ for the C–H_a oscillators and $\omega_e - \omega_e x_e = 3051$ cm^{-1} and $\omega_e x_e = -72$ cm^{-1} for the C–H_b oscillators. Studies of higher overtones ($\Delta\upsilon = 7, 8$) in the gas phase will probably show a better separation of the bands and will allow the determination of better spectroscopic constants. In order to do that, the sensitivity of the technique will have to be increased because the absorption cross sections at those levels are very small and the vapor pressure of trimethylborate is only 98 Torr at room temperature.

E. Molecular-orbital interactions

At first sight, the differences in the in-plane and out-of-plane C–H bond lengths and strengths in the $(CH_3O)_nBH_{3-n}$ series seem rather difficult to rationalize. However, the situation becomes somewhat clearer when the trends for the in-plane and out-of-plane C–H bonds are analyzed separately. The changes in the in-plane bonds can be attributed to interactions among the σ orbitals, and the changes in the out-of-plane bonds to the π orbital interactions.

1. π orbital interactions

The approximate group orbital energies for the π orbitals of $(CH_3O)_nBH_{3-n}$ are shown in Fig. 8(a). In CH_3OBH_2, the oxygen p_π lone pair interacts with the boron p_π orbital and is stabilized. This reduces its ability to interact with the CH_2 π^* group orbital. In $(CH_3O)_2BH$, the symmetric combination of the two oxygen p_π lone pairs interacts with the boron p_π orbital and is stabilized by about the same amount as in CH_3OBH_2. The antisymmetric combination of the two oxygen p_π lone pairs has a node at the boron; hence it is not stabilized and can interact more strongly with the CH_2 π^* group orbitals, lengthening the CH_b bonds relative to CH_3OBH_2. In $(CH_3O)_3B$, the symmetric (A) combination of the three oxygen p_π lone pairs is again stabilized by interaction with the boron p_π orbital. The two antisymmetric orbitals (E) are not stabilized and interact more strongly with the CH_2 π^* group orbitals, lengthening the out-of-plane bonds somewhat more than in $(CH_3O)_2BH$. Thus the lengthening of the out-of-plane bonds in the $(CH_3O)_nBH_{3-n}$ series can be attributed to increased oxygen p_π–CH_2 π^* interaction as the number of methoxy groups increases.

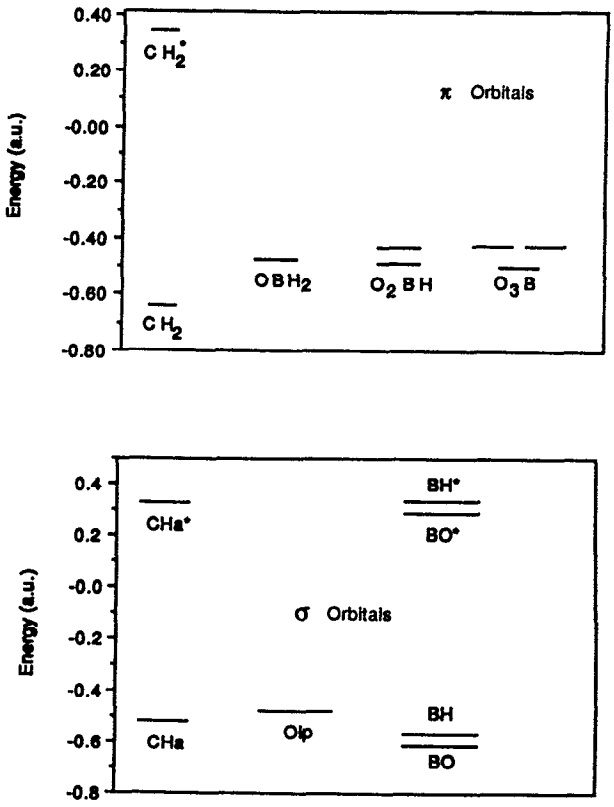

FIG. 8. Approximate energies for the π group orbitals (a) and σ group orbitals (b) of $(CH_3O)_nBH_{3-n}$ calculated at the HF/3-21G level.

2. σ orbital interactions

The approximate group orbital energies for the σ orbitals of $(CH_3O)_nBH_{3-n}$ are shown in Fig. 8(b). The interactions among these orbitals are a little more complicated than the π system, but also lead to discernible changes in bond lengths. The sp^2 lone pair of oxygen interacts more strongly with anti-periplanar bonds than with a syn-periplanar bond; the interaction lengthens the bond by donation into the σ^* orbital. In CH_3OBH_2, this causes the anti B–H bond to be longer than the syn B–H. Likewise in $(CH_3O)_2BH$, the B–O_2 bond that is anti to the O_1 lone pair is longer than the B–O_1 bond that is syn to the O_2 lone pair.

In $(CH_3O)_3B$, all of the B–O bonds are longer [relative to $(CH_3O)BH_2$], because each is anti to a lone pair. On the other hand, an oxygen lone pair that is anti to a B–H bond rather than a B–O bond is better able to interact with an anti C–H bond: The oxygen lone pair is pushed up more by the four electron destabilizing interaction with the higher-lying B–H σ orbital than with the lower-lying B–O σ orbital (and/or, the oxygen lone pair is not pushed down as much by the higher-lying B–H σ^* than by the lower-lying B–O σ^*). Thus an oxygen sp^2 lone pair anti to a B–H bond can interact more strongly with an anti C–H σ^* orbital, thereby lengthening the C–H bond. Consequently, the in-plane CH_a of $(CH_3O)BH_2$ and CH_{a1} of $(CH_3O)_2BH$ are longer than the CH_a of $(CH_3O)_3B$ and the CH_{a2} of $(CH_3O)_2BH$.

V. CONCLUSIONS

The spectra of C–H overtones of trimethylborate have been investigated in the liquid and gas phases. The combination band $\upsilon\upsilon(CH) + \upsilon_{19}$ observed for all the transitions from $\upsilon = 2$–6 shows a strong interaction between the C–H and the B–O stretching modes. The separation between bands of nonequivalent C–H bonds is very small and the bands are so wide that overlaped absorptions are obtained for overtones up to $\upsilon = 6$. Even though the *trans* effect has been used successfully to explain the results in molecules which contain a methyl group directly attached to an oxygen atom, it cannot be used to explain the results of the present work. *Ab initio* calculations of the molecular structure of $(CH_3O)_3B$ indicate that there are three equivalent in-plane CH bonds ($C–H_a$) and three equivalent pairs of out-of-plane CH bonds ($C–H_b$). The $C–H_a$ bonds are shorter than the out-of-plane $C–H_b$ bonds and correspondingly the stretching force constant for the $C–H_a$ is larger than for $C–H_b$. A study of orbital interactions in the series of molecules $(CH_3O)_nBH_{3-n}$ shows that the σ orbital interactions produce the changes in the in-plane $C–H_a$ bonds and the π orbital interactions produce the changes in the out-of-plane $C–H_b$ bonds.

ACKNOWLEDGMENT

This work was supported by the Robert A. Welch Foundation under Grant No. AA-1173.

[1] G. Gundersen, J. Mol. Struct. **33**, 79 (1976).
[2] A. Rogstad, B. N. Cyvin, S. J. Cyvin, and J. Brunvoll, J. Mol. Struct. **35**, 121 (1976).
[3] Y. Kawashima, H. Takeo, and C. Matsumura, J. Mol. Spectrosc. **116**, 23 (1986).
[4] D. C. McKean, Chem. Soc. Rev. **7**, 399 (1978), and references therein.
[5] H. L. Fang, D. M. Meister, and R. L. Swofford, J. Phys. Chem. **88**, 410 (1984); **88**, 405 (1984).
[6] H. L. Fang, R. L. Swofford, and D. A. C. Compton, Chem. Phys. Lett. **108**, 539 (1984).
[7] L. J. Bellamy and D. W. Mayo, J. Phys. Chem. **80**, 1217 (1976).
[8] L. J. Bellamy, *The Infrared Spectra of Complex Molecules, Vol. 2, Advances in Infrared Group Frequencies*, 2nd ed. (Chapman and Hall, New York, 1980).
[9] J. S. Wong and C. B. Moore, J. Chem. Phys. **77**, 603 (1982).
[10] M. D. Harmony, V. W. Laurie, R. L. Kuczkowski, R. H. Schwendeman, D. A. Ramsay, F. J. Lovas, W. J. Lafiarty, and A. G. Maki, J. Phys. Chem. Ref. Data **8**, 619 (1979).
[11] R. F. Curl, J. Chem. Phys. **30**, 1529 (1959).
[12] P. N. Ghosh, A. Bauder, and Hs. H. Gunthard, Chem. Phys. **53**, 39 (1980).
[13] A. P. Cox and S. Waring, Faraday Trans. Soc. **67**, 3441 (1971).
[14] J. S. Ridgen and S. S. Butcher, J. Chem. Phys. **40**, 2109 (1964).
[15] R. Mecke and R. Ziegler, Z. Phys. **101**, 405 (1936).
[16] G. Herzberg, *Infrared and Raman Spectra* (Van Nostrand, New York, 1945).
[17] B. R. Henry, Acc. Chem. Res. **10**, 207 (1976).
[18] A. B. Burg and H. I. Schlesinger, J. Am. Chem. Soc. **55**, 4020 (1933).
[19] D. G. Cameron, D. Scolar, L. Kompa-Krymien, P. Neelakanton, and R. N. Jones, Natl. Res. Counc. Can., Bull. No. 14, Ottawa (1976).
[20] R. N. Jones and J. Pitha, Natl. Res. Counc. Can. Bull. No. 12, Ottawa (1968).
[21] J. S. Binkley, M. J. Frisch, D. J. DeFrees, K. Raghavachari, R. A. Whiteside, H. B. Schlegel, D. J. Fox, R. L. Martin, E. M. Fleuder, C. F. Melius, L. R. Kahn, J. J. P. Steward, F. W. Bobrowicz, and J. A. Pople, GAUSSIAN 86, Carnegie-Mellon University, Pittsburgh, PA (1984).
[22] H. B. Schlegel, J. Comput. Chem. **3**, 214 (1982).
[23] J. S. Binkley and J. A. Pople, Theor. Chim. Acta **28**, 213 (1973).
[24] J. A. Pople, R. Krishnan, H. D. Schlegel, and J. S. Binkley, Int. J. Quantum Chem., Quantum Chem. Symp. **13**, 225 (1979).
[25] The structural parameters were determined by a least-squares fitting of a series of rotational constants obtained from the microwave study of the deuterated species $CH_nD_{3-n}OBH_2$. In the fits, the B–H lengths were constrained to be equivalent and equal to the value obtained from the *ab initio* calculation at the 4-31G* level (see Ref. 3). In addition, the ratio R(B–O)/R(C–O) was assumed to be equal to the ratio obtained at the 4-31G* level of theory.
[26] A. L. Aljibury, R. G. Snyder, H. L. Strauss, and K. Raghavachari, J. Chem. Phys. **84**, 6872 (1986).
[27] M. L. Sage, J. Chem. Phys. **80**, 2872 (1984).
[28] C. Manzanares, N. L. S. Yamasaki, and E. Weitz, J. Phys. Chem. **91**, 3959 (1987).
[29] R. T. Birge and H. Sponer, Phys. Rev. **28**, 259 (1926).